



Cite this: *Chem. Commun.*, 2016, 52, 394

Received 17th July 2015,
Accepted 24th October 2015

DOI: 10.1039/c5cc05801e

www.rsc.org/chemcomm

The association and aggregation of the metamorphic chemokine lymphotactin with fondaparinux: from nm molecular complexes to μm molecular assemblies†

Sophie R. Harvey,^a Cait E. MacPhee,^b Brian F. Volkman^c and Perdita E. Barran^{*d}

Transmission electron microscopy, mass spectrometry, and drift tube ion mobility-mass spectrometry are used to study the assemblies formed by the metamorphic chemokine lymphotactin in the presence of a model pentameric glycosaminoglycan, fondaparinux. This combination of techniques delineates significant differences in the complexes observed for two forms of the full length protein as well as a truncated form, without the intrinsically disordered C-terminal tail, over a length scale from few nm to μm assemblies.

The chemokine lymphotactin (Ltn) is a metamorphic protein which exists in equilibrium between two distinct conformations, and contains only a single disulfide bond as opposed to the two normally found in chemokines.^{1,2} The first form is a monomeric form which adopts the conserved chemokine fold, and is known as Ltn10.³ The second form is a unique dimeric fold, known as Ltn40.⁴ Both Ltn10 and Ltn40 contain a structural core and an, extended, intrinsically disordered (ID) C-terminal tail, which is distinctive of this chemokine.

Chemokines fulfil their biological function through high-affinity interactions with cell-surface G protein coupled receptors (GPCRs).⁵ Recent studies, however, have shown these proteins also exhibit low-affinity interactions with glycosaminoglycans (GAGs) present on cell surfaces or in the extracellular matrix.^{6,7} Chemokines are hypothesized to bind GAGs as a localisation mechanism, in order to act as a directional signal for migrating cells.⁸ The functional importance of such interactions was reinforced with an influential study by Proudfoot *et al.*⁹ where site specific mutations were engineered to inhibit GAG binding and found *in vitro* to minimally perturb receptor binding. *In vivo*, however, these mutants were ineffective at inducing cell migration in comparison

to the WT chemokine, attributed to the necessity of specific chemokine:GAG interactions and resulting chemokine aggregation. The resulting aggregation is deemed essential and thought to help over-come issues associated with vascular flow.¹⁰ Despite this to-date, to the best of our knowledge, there have been no reports of using transmission electron microscopy (TEM), as a biophysical technique, to study the aggregation of chemokines occurring in the presence of GAGs *in vitro*. Here we have utilised both TEM and drift tube ion mobility-mass spectrometry to study the interactions between Ltn and a model pentameric GAG, fondaparinux (Fx).

Wild type (WT) Ltn was studied by TEM in the absence and presence of Fx after incubation at room temperature for 30 minutes (Fig. 1A and B). WT Ltn exhibits limited aggregation in the absence of Fx (Fig. 1A), however, extensive aggregation is observed in the presence of Fx (Fig. 1B). The morphology of the aggregates are striking, forming large, ordered, ribbon-like species over 10 μm long, and approximately 0.2 μm wide. These sizes along with the homogeneity of the ribbons, are also remarkable when considering the relatively short incubation time. In addition, Fx also shows only limited signs of aggregation in the absence of Ltn (Fig. S1, ESI†) highlighting that this aggregation is due to the presence, and interactions, of both Ltn and Fx.

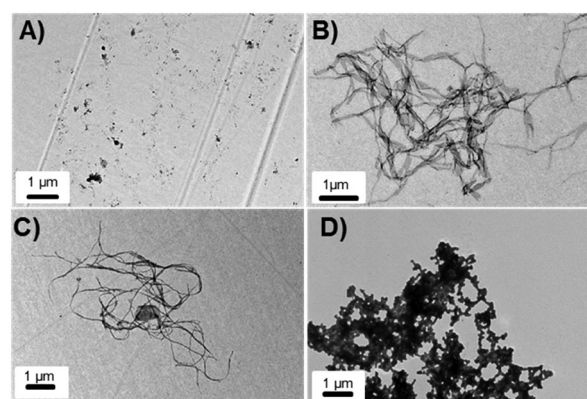


Fig. 1 TEM images acquired for (A) WT Ltn, and from 1:1 mixtures of Ltn and Fx for (B) WT, (C) CC3 and (D) WT 1–72 prepared in 20 mM ammonium acetate.

^a School of Chemistry, University of Edinburgh, West Mains Road, EH8 3JJ, Edinburgh, UK

^b School of Physics and Astronomy, University of Edinburgh, West Mains Road, EH9 3JZ, Edinburgh, UK

^c Department of Biochemistry, Medical College of Wisconsin, Milwaukee, WI 53226, USA

^d School of Chemistry, Manchester Institute of Biotechnology, University of Manchester, M1 7DN, UK. E-mail: Perdita.barran@Manchester.ac.uk

† Electronic supplementary information (ESI) available: Experimental conditions, additional figures. See DOI: 10.1039/c5cc05801e



The GAG binding functionality of Ltn has been previously, assessed *via* elution from a heparin-sepharose column with a sodium chloride gradient.¹¹ WT Ltn was found to elute in two broad fractions which were assigned as the two conformations (Ltn10 and Ltn40) of WT Ltn having significantly different binding affinities, with Ltn40 having the higher binding affinity. Due to the fact that monomeric, Ltn10 is thought to have a lower binding affinity for GAGs, we also studied a stabilised monomeric mutant of Ltn (CC3). CC3 is a constrained form of Ltn with an additional disulfide bond placed to limit interconversion between the monomeric and dimeric forms;¹² the extra disulphide bridge gives rise to a structure more akin to classic chemokines. Following incubation with Fx, CC3 is observed to behave in a similar fashion to the WT Ltn (Fig. 1C). For the CC3 mutant, there are also ribbon-like structures but these are much narrower ~50 nm than for the wild type, suggesting that when the tail is partially tethered by the additional disulphide bridge the growth across the width of the ribbon is restricted. The clusters of ribbons formed are also not as numerous or extensive as in the WT:Fx mixture, suggesting either this species has a significantly lower affinity for the grid or that CC3:Fx aggregates to a lesser extent. Lower affinity binding, resulting in less aggregation, is consistent with the previous heparin-sepharose column studies in which CC3 eluted in a single fraction, corresponding with the lower affinity fraction of the WT Ltn (Ltn10).¹¹

One of the distinctive features of Ltn, in comparison to other chemokines, is that it contains an extended, highly flexible, C-terminal tail, here we examine a construct which comprises only the structural core and not the ID tail, known as WT 1–72 (Fig. 1D). The TEM images obtained when incubated with Fx are significantly different to those obtained from the WT and CC3, suggesting different interactions and growth processes *in vitro*. The truncated WT 1–72 does not produce ribbons at all, rather larger globular aggregates, strikingly different in appearance. Classic chemokines, have not been studied previously in the presence of GAGs by TEM, so which morphology (ribbon-like or globular) these species would adopt is as yet unknown but this data suggests that they would behave like the WT 1–72, since they do not possess an ID tail. Furthermore since the functional role of the Ltn tail is currently under debate and it has been found to be completely dispensable for receptor binding,¹² the fact that notably different behaviour with respect to GAG binding indicates a new role. The significant differences in aggregate morphology could stem from differences in the association at the monomer or dimer level. Therefore, in order to better understand the early stages of aggregation, that may influence the differences in the aggregated structures, we turned to native-like mass spectrometry, and drift-tube ion mobility-mass spectrometry (DT IM-MS).

Both MS and IM-MS have previously been used to examine interactions between proteins and GAGs,^{13–17} enabling even low intensity complexes to be separated and identified. Furthermore MS is inherently well suited to the study of aggregating systems.^{18–21} The combination of MS with DT IM-MS studies provides additional information on the size and shape of the ions, in the form of rotationally averaged collision cross sections (CCS). Determination of CCS for proteins,^{22,23} protein:protein complexes^{24,25} and chemokine:GAG complexes^{26,27} has provided insight into these essential biomolecules.

The spectra previously obtained for these Ltn constructs in the absence of Fx, demonstrate that all three exist primarily in a monomeric (M) form (Fig. S2, ESI†).^{28,29} For WT Ltn a significant proportion of dimer (D) is also observed. In the presence of a stoichiometric concentration of Fx, both WT and CC3 bind Fx primarily in their monomeric (M) form (Fig. 2A and B), with unbound monomeric protein remaining the most intense observable species. In addition, lower intensity dimeric Ltn:Fx complexes are observed for both WT and CC3. Based on previous heparin-sepharose column studies it was anticipated that the dimeric form of WT Ltn would bind Fx to a greater extent than the monomeric form. It is possible that the monomeric species is formed faster or is an encounter species *en route* to the dimer bound species. It proved impossible to test this theory with MS, as upon addition of Fx to Ltn extensive aggregation occurs, with large aggregates visible in the n-ESI tip (Fig. S3, ESI†). The solution changes from clear to cloudy in appearance, typically over the course of one hour, and is accompanied by a significant reduction in signal intensity, consistent with the rapid formation of large aggregates as observed in the TEM images (Fig. 1). We assessed the specificity of Ltn to form monomeric and dimeric Fx bound species as a function of concentration; at all concentrations both monomeric and dimeric complexes are observed (Fig. S4, ESI†). $M_{WT} + Fx$ species are present at all concentrations studied, suggesting these complexes are specific and are formed in equilibrium with $D_{WT} + Fx$. For CC3 the fact that the most intense GAG-bound species is $M_{CC3} + Fx$ with lower relative

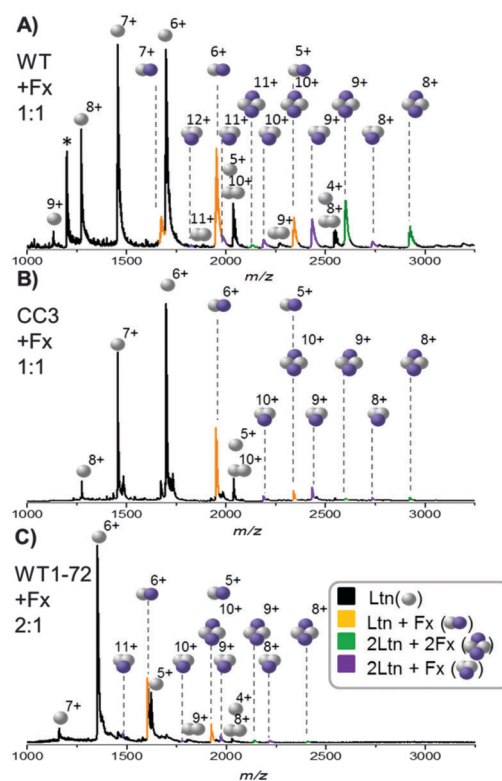


Fig. 2 nESI mass spectra acquired from a 1 : 1 mixture of Ltn plus Fx, at 50 μ M protein concentration in 20 mM ammonium acetate (A) WT ltn (B) CC3 and at a 2 : 1 (Ltn:Fx) concentration at 25 μ M protein concentration in 20 mM ammonium acetate for (C) structural core, WT 1–72. * denotes a contaminant.



intensity of dimeric bound species is unsurprising considering this is a stabilized monomeric construct of Ltn. Whereas, WT Ltn which exists in equilibrium between the monomer and the dimer has a significant GAG-bound population of both. Furthermore, the low intensity dimer bound species observed are consistent with other chemokines in which the presence of GAGs increases the proportion of higher order oligomers and which have been shown to bind GAGs as monomers, dimers or even tetramers.^{27,30} For both WT and CC3 these $2[\text{protein}] + n[\text{GAG}]$ species could, therefore, be the growth competent blocks for the large aggregates observed in TEM.

The structural core of Ltn (WT 1–72) displays remarkably different behaviour by MS in the presence of Fx. A stoichiometric mixture at 50 μM resulted in extensive aggregation, evidenced by a raised baseline in the spectrum (Fig. S5, ESI†), poor signal-to-noise, and extensive visual signs of aggregation in the nESI capillaries. All of which are consistent with extensive aggregation. Again akin to the aggregation observed by TEM. This system was reanalysed at a 2 : 1 (Ltn : Fx) ratio (25 μM Ltn) (Fig. 2C). As for WT and CC3, WT 1–72 forms monomeric ($M_{1-72} + \text{Fx}$) and dimeric ($D_{1-72} + \text{Fx}$ and $D_{1-72} + 2\text{Fx}$) Fx bound complexes. The considerable increase in aggregation observed for 1–72 in comparison with WT and CC3, both by TEM and MS, implies the ID tail may act to inhibit GAG binding and subsequent aggregation. As a control the ID tail itself was also studied in the absence and presence of Fx by MS (Fig. S6, ESI†) and no Fx binding was observed, implying that the tail itself does not contain or configure the GAG binding site(s), which is consistent with the lower proportion of basic residues here.

Given the differences between the full length (WT and CC3) and truncated (WT 1–72) constructs, both in MS and with respect to the aggregate morphologies we then considered the conformation of the Ltn:Fx complexes using DT IM-MS. We have previously studied these Ltn constructs by DT IM-MS and determined their $^{\text{DT}}\text{CCS}_{\text{He}}$ in the absence of Fx,^{28,29} enabling comparisons between the Fx bound and unbound species to be made at the same charge state (Fig. 3 and Table S1, ESI†). For both WT and CC3 (Fig. 3A and B) Fx binding reduces the absolute CCS for $[M + \text{Fx} + 5\text{H}]^{5+}$ and shows very little change in CCS (which given the mass increase is an effective decrease) for $[M + \text{Fx} + 6\text{H}]^{6+}$. For the unbound species, at the same charge states, previous studies suggested the compact $^{\text{DT}}\text{CCS}_{\text{He}}$ were due to the ID tail being associated or wrapped around the structural core with a major increase in $^{\text{DT}}\text{CCS}_{\text{He}}$ observed when the tail unfolds,^{28,29} hence it is thought that the low $^{\text{DT}}\text{CCS}_{\text{He}}$ calculated for the GAG-bound species here are also due to the ID tail being associated with the core. It is expected that electrostatic forces will play a role in the binding of GAGs to chemokines, as GAGs are highly negatively charged and chemokines are basic proteins. These forces will in part account for the tight conformations observed here for CC3 and WT, consistent with previous studies which report compaction with GAG chemokine complexes.²⁷

The $^{\text{DT}}\text{CCS}_{\text{He}}$ of $[M_{\text{WT}} + \text{Fx} + 7\text{H}]^{7+}$, however, is significantly larger than both its unbound counterpart and the bound species of lower charge state, with a 50% increase in the $^{\text{DT}}\text{CCS}_{\text{He}}$ for the $[M_{\text{WT}} + \text{Fx} + 7\text{H}]^{7+}$ compared with $[M_{\text{WT}} + \text{Fx} + 5\text{H}]^{5+}$ (1247 vs. 845 \AA^2). This shows that the Ltn:Fx complex is capable of adopting a wide range of conformations. Considering the inherent flexibility of Ltn, it is likely that this protein will form complexes with different specific

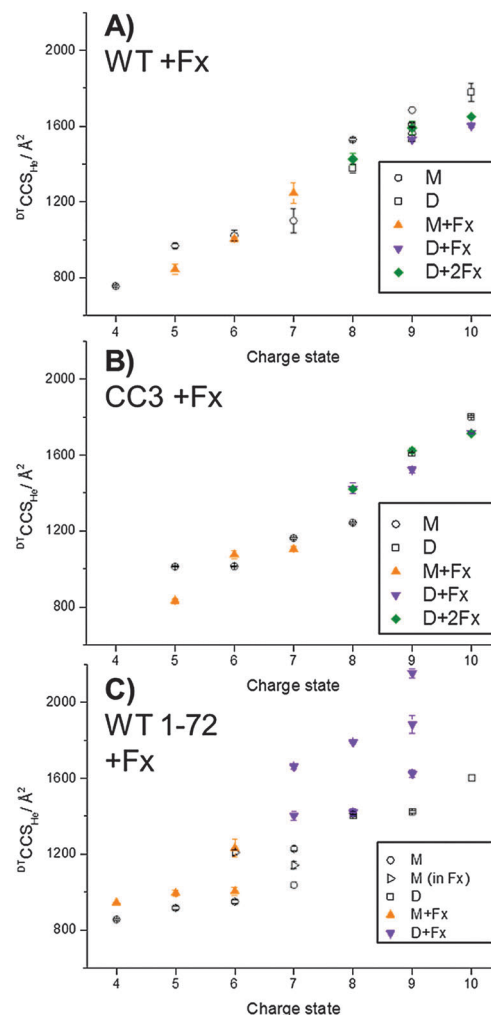


Fig. 3 Average $^{\text{DT}}\text{CCS}_{\text{He}}$ calculated from three repeats (Table S1, ESI†), error bars represent standard deviation between these values and often fall within symbol size. Unbound species $^{\text{DT}}\text{CCS}_{\text{He}}$ were determined in absence of Fx.^{28,29} For WT 1–72 significant differences in $^{\text{DT}}\text{CCS}_{\text{He}}$ for the unbound species were observed in presence of Fx, for these species $^{\text{DT}}\text{CCS}_{\text{He}}$ are shown with a right handed triangle. For figure clarity only charge states in which both bound and unbound protein are observed are shown.

conformations. This increase in $^{\text{DT}}\text{CCS}_{\text{He}}$ is not observed for $[M_{\text{CC3}} + \text{Fx} + 6\text{H}]^{6+}$ implying decreased conformational flexibility for this constrained construct. Furthermore, for both full length constructs the $^{\text{DT}}\text{CCS}_{\text{He}}$ of the dimeric form complexed with one or two Fx gives highly similar values to the unbound dimer or are even more compact, consistent with a conformational tightening upon binding, potentially forming the core aggregating unit resulting in similar morphologies.

For both CC3 and WT Ltn the conformations of the dimeric bound species are not observed to change substantially with charge, increasing by a maximum by 21%, and do not change substantially upon binding a second Fx chain. This observation suggests that the individual proteins exist in a single, stable conformational family upon Fx binding.

The $^{\text{DT}}\text{CCS}_{\text{He}}$ of the Fx bound WT 1–72 tell a dramatically different story to the full length WT Ltn (Fig. 3C, and Table S1 ESI†).



For WT 1–72 multiple conformations are observed for both the $M_{1-72} + \text{Fx}$ and the $D_{1-72} + \text{Fx}$ species. The $D_{1-72} + 2\text{Fx}$ species were not observed at a high enough intensity to enable determination of $^{\text{DT}}\text{CCS}_{\text{He}}$. The $^{\text{DT}}\text{CCS}_{\text{He}}$ determined for $M_{1-72} + \text{Fx}$ species are larger than their unbound counterparts. Whilst, the $D_{1-72} + \text{Fx}$ species adopt multiple conformations, the more compact of which has a similar $^{\text{DT}}\text{CCS}_{\text{He}}$ to D_{1-72} at the same charge state, however, the second conformational family has a much larger $^{\text{DT}}\text{CCS}_{\text{He}}$ than the unbound species. Furthermore, for $[D_{1-72} + \text{Fx} + 9\text{H}]^{9+}$ a third, more extended, conformation is also observed, attributable to Coloumbic repulsion. The observation of multiple conformations, in combination with the extensive amorphous aggregation observed by TEM (Fig. 1D) suggests binding for WT 1–72 is more complex than for WT and CC3. It is surmised that the tail is needed to mediate binding and in doing so, also confers a conformational stability to the complexes and provides a more structurally homogenous core from which aggregation may proceed.

It is interesting to note that for both WT and CC3 the $^{\text{DT}}\text{CCS}_{\text{He}}$ the unbound species determined in the absence and presence of Fx are within error (Tables S2 and S3, ESI[†]). In contrast, however, in the presence of Fx the unbound 6+ and 7+ monomeric WT 1–72 species are present with larger $^{\text{DT}}\text{CCS}_{\text{He}}$ implying that the GAG induces a conformational change to the protein core (Table S4, ESI[†]), it is possible these species are *en route* to complex formation or have transient, weaker interactions in resulting in ligand loss upon on transfer to the gas phase. Considering the electrostatic nature of these interactions, however, along with the gentle desolvation, ionisation, and transfer conditions used here it is unlikely that substantial ligand dissociation would occur.

In conclusion, this work has shown that despite its structural metamorphosis the functions of WT Ltn are not completely separate and defined *in vitro* and Ltn is capable of binding Fx as both a monomer and a dimer. Both WT Ltn and a constrained monomer mutant display similar behaviour in the presence of Fx, while a construct without the ID tail (WT 1–72) behaves significantly differently with more extensive rapid aggregation occurring, forming large globular species. The similar trends in conformations adopted by the soluble aggregates for WT and CC3 are interesting to note when considering the similar morphologies of the large, insoluble aggregates observed by TEM. In contrast WT 1–72 displays significantly different behaviour, as viewed by DT IM-MS, the wide range of extended conformations determined for this construct suggest binding is less specific in this case. This less specific binding could explain the striking differences in aggregate morphology seen in TEM. It is therefore probable that the species observable in MS and DT IM-MS are *en route* to aggregate formation.

Based on the results for WT 1–72 in comparison to all full length constructs, it is suggested that the ID tail mediates aggregation and binding, proposing a previously unknown structural role for this region. We have shown here that the diversity in the CCS of complex conformers at the molecular level correlates with the diversity in the morphology of the μm scale aggregates. Clearly, GAG binding is a complicated and intricate process, however, the combination of biophysical tools utilised here can probe this in detail *in vitro*.

The Schools of Chemistry and Physics at the University of Edinburgh are thanked for the award of an EPSRC DTA studentship

to SRH. The EPSRC and the University of Manchester are thanked for the award of a postdoctoral prize fellowship to SRH. Steve Mitchell is gratefully acknowledged for his help in operating the TEM. The BBSRC are also thanked for awards BB/L015048/1 and BB/H013636/1 which have funded the continuation of this work.

References

- G. S. Kelner, J. Kennedy, K. B. Bacon, S. Kleyensteuber, D. A. Largaespa, N. A. Jenkins, N. G. Copeland, J. F. Bazan, K. W. Moore and T. J. Schall, *Science*, 1994, **266**, 1395–1399.
- C. Chemokine, *J. Interferon Cytokine Res.*, 2002, **22**, 1067–1068.
- E. S. Kuloglu, D. R. McCaslin, M. Kitabwalla, C. D. Pauza, J. L. Markley and B. F. Volkman, *Biochemistry*, 2001, **40**, 12486–12496.
- R. L. Tuinstra, F. C. Peterson, S. Kutlesa, E. S. Elgin, M. A. Kron and B. F. Volkman, *Proc. Natl. Acad. Sci. U. S. A.*, 2008, **105**, 5057–5062.
- T. Handel and D. Hamel, *Chemokines*, Academic Press, 2009.
- T. M. Handel, Z. Johnson, S. E. Crown, E. K. Lau and A. E. Proudfoot, *Annu. Rev. Biochem.*, 2005, **74**, 385–410.
- Z. Johnson, A. Proudfoot and T. Handel, *Cytokine Growth Factor Rev.*, 2005, **16**, 625–636.
- D. J. Hamel, A. E. Proudfoot and T. M. Handel, *Methods Enzymol.*, 2009, **461**, 71–102.
- A. E. I. Proudfoot, T. M. Handel, Z. Johnson, E. K. Lau, P. LiWang, I. Clark-Lewis, F. Borlat, T. N. C. Wells and M. H. Kosco-Vilbois, *Proc. Natl. Acad. Sci. U. S. A.*, 2003, **100**, 1885–1890.
- S. J. Allen, S. E. Crown and T. M. Handel, *Annu. Rev. Immunol.*, 2007, **25**, 787–820.
- B. F. Volkman, T. Y. Liu and F. C. Peterson, *Methods Enzymol.*, 2009, **461**, 51–70.
- R. L. Tuinstra, F. C. Peterson, E. S. Elgin, A. J. Pelzek and B. F. Volkman, *Biochemistry*, 2007, **46**, 2564–2573.
- Y. Yu, M. D. Sweeney, O. M. Saad, S. E. Crown, T. M. Handel and J. A. Leary, *J. Biol. Chem.*, 2005, **280**, 32200–32208.
- Y. Yu, M. D. Sweeney, O. M. Saad and J. A. Leary, *J. Am. Soc. Mass Spectrom.*, 2006, **17**, 524–535.
- M. D. Sweeney, Y. Yu and J. A. Leary, *J. Am. Soc. Mass Spectrom.*, 2006, **17**, 1114–1119.
- E. S. Seo, B. S. Blaum, T. Vargues, M. De Cecco, J. A. Deakin, M. Lyon, P. E. Barran, D. J. Campopiano and D. Uhrin, *Biochemistry*, 2010, **49**, 10486–10495.
- I. C. Severin, J. P. Gaudry, Z. Johnson, A. Kungl, A. Jansma, B. Gesslbauer, B. Mulloy, C. Power, A. E. Proudfoot and T. Handel, *J. Biol. Chem.*, 2010, **285**, 17713–17724.
- S. L. Bernstein, T. Wyttenbach, A. Baumketner, J.-E. Shea, G. Bitan, D. B. Teplow and M. T. Bowers, *J. Am. Chem. Soc.*, 2005, **127**, 2075–2084.
- S. L. Bernstein, N. F. Dupuis, N. D. Lazo, T. Wyttenbach, M. M. Condrón, G. Bitan, D. B. Teplow, J.-E. Shea, B. T. Ruotolo, C. V. Robinson and M. T. Bowers, *Nat. Chem.*, 2009, **1**, 326–331.
- A. M. Smith, T. R. Jahn, A. E. Ashcroft and S. E. Radford, *J. Mol. Biol.*, 2006, **364**, 9–19.
- H. L. Cole, J. M. D. Kalapothakis, G. Bennett, P. E. Barran and C. E. MacPhee, *Angew. Chem.*, 2010, **122**, 9638–9641.
- K. B. Shelimov, D. E. Clemmer, R. R. Hudgins and M. F. Jarrold, *J. Am. Chem. Soc.*, 1997, **119**, 2240–2248.
- D. E. Clemmer, R. R. Hudgins and M. F. Jarrold, *J. Am. Chem. Soc.*, 1995, **117**, 10141–10142.
- M. Zhou, S. Dagan and V. H. Wysocki, *Angew. Chem., Int. Ed.*, 2012, **51**, 4336–4339.
- C. Uetrecht, I. M. Barbu, G. K. Shoemaker, E. van Duijn and A. J. Heck, *Nat. Chem.*, 2011, **3**, 126–132.
- M. R. Schenauer and J. A. Leary, *Int. J. Mass Spectrom.*, 2009, **287**, 70–76.
- Y. Seo, A. Andaya, C. Bleiholder and J. A. Leary, *J. Am. Chem. Soc.*, 2013, **135**, 4325–4332.
- S. R. Harvey, M. Porini, A. Konijnenberg, D. J. Clarke, R. C. Tyler, P. R. R. Langridge-Smith, C. E. MacPhee, B. F. Volkman and P. E. Barran, *J. Phys. Chem. B*, 2014, **118**, 12348–12359.
- S. R. Harvey, M. Porini, R. C. Tyler, C. E. MacPhee, B. F. Volkman and P. E. Barran, *Phys. Chem. Chem. Phys.*, 2015, **16**, 10538–10550.
- A. L. Jansma, J. P. Kirkpatrick, A. R. Hsu, T. M. Handel and D. Nietlispach, *J. Biol. Chem.*, 2010, **285**, 14424–14437.

